Journal of Power Sources 196 (2011) 9473–9480

Contents lists available at ScienceDirect

Journal of Power Sources

journal homepage: www.elsevier.com/locate/jpowsour

Analytical model to relate DMFC material properties to optimum fuel efficiency and system size

Jeremy P. Meyers*, Brent Bennett

Department of Mechanical Engineering/The Center for Electrochemistry, The University of Texas at Austin, Austin, TX 78712, USA

ARTICLE INFO

Article history:
Received 27 April 2011
Received in revised form 2 July 2011
Accepted 5 July 2011
Available online 12 July 2011

Keywords:
Fuel cells
Analysis
Methanol
Material properties
System optimization

ABSTRACT

In the design of the direct methanol fuel cell and the evaluation of new materials and their appropriateness for inclusion, it is helpful to consider the impact of material properties on the performance of a complete system: to some degree, methanol crossover losses can be mitigated by proper system design. As such, an analytical model is developed to evaluate the methanol concentration profile across the anode backing layer and membrane of the direct methanol fuel cell. The model is integrated down the anode flow channel to determine fuel utilization as a function of the feed concentration, backing layer properties, and membrane properties. A minimum stoichiometric ratio is determined based on maintaining zero-order methanol kinetics, which allows the fuel efficiency to be optimized by controlling these physical properties. This analysis is then used to estimate the required flow rates and the size of system components such as the methanol storage tank, based on the minimum methanol flow rate that those components must produce to deliver a specified current; in this way, the system-level benefits of reduced membrane crossover can be evaluated.

1. Introduction

The direct methanol fuel cell (DMFC) is an electrochemical energy conversion device that operates by converting methanol and water to carbon dioxide and protons at the anode, $CH_3OH + H_2O \leftrightarrows CO_2 + 6H^+ + 6e^-$, and by reducing oxygen at the cathode, $O_2 + 4H^+ + 4e^- \leftrightarrows 2H_2O$. The primary advantage of the DMFC is that it can be operated with a liquid feed, and therefore does not require a reformer or a bulky gas storage tank. Also, because the oxidation reaction produces six electrons per methanol molecule, the DMFC delivers a high specific energy. The simplicity and compactness of the fuel delivery system makes the DMFC attractive for portable applications.

A paramount problem in the implementation of the DMFC is methanol crossing over to the cathode, where it is oxidized, resulting in a depolarization of the positive electrode and a waste of fuel. The origin of crossover lies in the fact that methanol is completely soluble in water and that water is needed to swell the proton-exchange membrane and to impart protonic conductivity across the membrane. One way to mitigate this problem is to create a low-crossover membrane to replace standard perflourosulfonic acid membranes such as Nafion®. Increasing the efficiency of the anode reaction through the design of the catalyst layer can also minimize crossover. Finally, optimizing the design of the anode flow channel and operating parameters such as methanol feed concentration and temperature is crucial.

During the past two decades, numerous approaches to modeling the DMFC have been taken. Most of these models are numerical or semi-empirical, with only a handful being analytic, and most focus on polarization, power output and/or kinetics. Among the analytical models, the majority are one-dimensional, single-phase models [1–14] with a few multi-dimensional models [15,16]. There are also many DMFC models that consider explicitly the engineering problems of fuel utilization and efficiency [17–27], but none of these are analytic in nature. There are also numerous models in the literature that consider crossover, including a majority of the analytic models [1–5,9,10,12,13,15], but these models do not consider the system-level problem of fuel utilization and its relationship to crossover.

In this paper, we seek to calculate the magnitude of methanol crossover for different membrane and backing layer properties when we design the system around optimized fuel efficiency. First, we develop analytical solutions for the methanol concentration in the anode flow channel, anode backing layer, and membrane based on the methanol feed concentration and the methanol mass transfer coefficients in the backing layer and membrane. We then set a minimum allowable stoichiometric ratio in order to ensure

* Corresponding author at: 1 University Station, C2200, Austin, TX 78712-0292, USA. Tel.: +1 512 232 5276; fax: +1 512 471 7681.
E-mail addresses: jeremypmeyers@mail.utexas.edu, jeremypmeyers@austin.utexas.edu (J.P. Meyers), brent-bennett@mail.utexas.edu (B. Bennett).

0378-7753/$ – see front matter © 2011 Published by Elsevier B.V.
doi:10.1016/j.jpowsour.2011.07.017

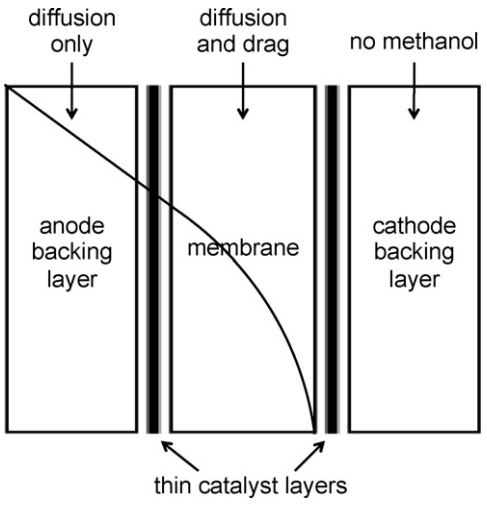

Fig. 1. Cross-section of the cell including a qualitative rendering of the methanol concentration profile.

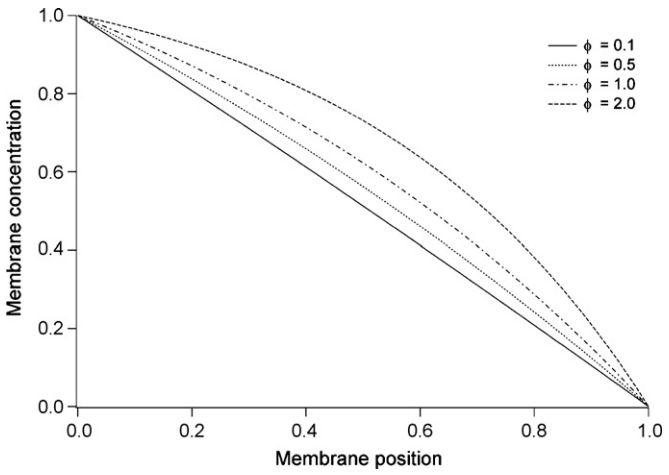

Fig. 2. Membrane concentration profile for different values of phi. The membrane concentration is normalized according to the anode concentration, and the membrane position is also normalized.

that the system is always operated with sufficiently high methanol concentrations so that the anode reaction remains zero-order with methanol concentration. The inverse of the stoichiometric ratio is the fuel efficiency, so by setting a minimum value on the amount of fuel delivered, we set a maximum value on the fuel efficiency. We are then able to optimize the membrane and backing layer properties to deliver the maximum possible fuel efficiency. Finally, we demonstrate how to determine the size of system components, especially the methanol storage tank, for a cell operating at its minimum stoichiometric ratio. The sizes of these components scale with the total flow rate of methanol into the cell, so by calculating the minimum flow rate corresponding to the maximum efficiency, we can estimate their minimum sizes.

It is important to note that this model is concerned only with methanol concentration and does not employ electrochemical equations to calculate polarization or power density. Therefore, we do not consider proton transport or the effects of ohmic losses in the membrane. Any effects stemming from water transport or carbon dioxide gas removal on the anode side are ignored or incorporated into an overall effective diffusion coefficient. The cathode is not considered explicitly because any methanol that reaches the cathode catalyst layer is assumed to be immediately oxidized. The methanol is assumed to be an ideal incompressible liquid in an isothermal environment such that any pressure or temperature effects can also be ignored. Much work has been done, most notably by Scott et al. [28] and Wang and Wang [29], to show that two-phase effects can be important even in primarily liquid-feed DMFCs, but this model, like previous analytical models, does not consider those effects. Instead, we assume that the behavior of the backing layer can be characterized simply by an effective diffusion coefficient and by its thickness.

2. Methanol concentration

2.1. Anode backing layer

The methanol concentration in the cell can be broken down into two orthogonal concentration profiles: the concentration profile across the thickness of the cell (Figs. 1 and 2) and the concentration profile down the flow channel as methanol is consumed through reaction and crossover (Figs. 3 and 4). To find the concentration profile in the anode backing layer, we first assume that any methanol entering the anode backing layer is either consumed in the desired reaction at the anode, thereby producing six electrons, or crosses over into the membrane. In the development of the model that follows, we assume that all fluxes and current densities are defined per unit of superficial area, and transport properties are effective transport properties, modified from bulk values by appropriate corrections for volume fraction and tortuosity. We also neglect convection across the thickness of the cell. Assuming the

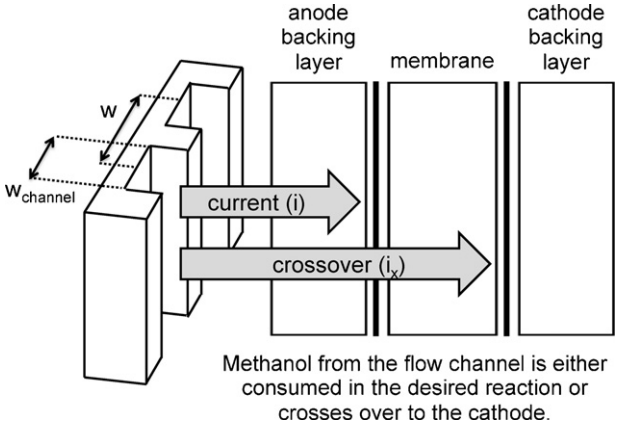

Fig. 3. Methanol consumption in the fuel cell.

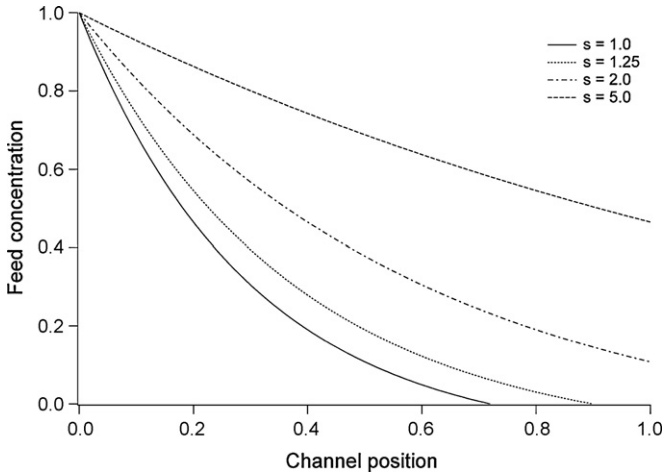

Fig. 4. Normalized feed concentration as a function of normalized distance down the channel with $\nu = 2$ and $\psi = 5$.

only transport mechanism at work in the backing layer is diffusion, the methanol flux density is

$$N_{\mathrm{MeOH}}^{backing} = \frac{i}{6F} + \frac{i_x}{6F} = \frac{D_{backing}}{L_{backing}}(c_{feed} - c_{anode}). \quad (1)$$

The flux is constant at steady state, so $\nabla \cdot N_{\mathrm{MeOH}}^{backing} = 0$, which implies that the resulting concentration profile in the backing layer is linear.

When the concentration at the anode goes to zero, the crossover current disappears, and the limiting current in the backing layer is

$$i_{\mathrm{lim}} = 6F\left(\frac{D_{backing}}{L_{backing}}\right) c_{feed}. \quad (2)$$

Therefore, the maximum rate of transport from the flow channel to the electrode and membrane is set by c_{feed}, which is the methanol concentration in the flow channel, and the backing layer properties $D_{backing}$ and $L_{backing}$. The crossover current can now be described as a function of this limiting current

$$i_x = 6F\left(\frac{D_{backing}}{L_{backing}}\right)(c_{feed} - c_{anode}) - i = i_{\mathrm{lim}}\left(\frac{c_{feed} - c_{anode}}{c_{feed}}\right) - i. \quad (3)$$

2.2. Membrane

We assume that the concentration of methanol at the cathode is driven to zero, and define the current as positive (from the anode toward the cathode) because the oxidation reaction is occurring at the anode. In order to keep this model as simple as possible, we choose to ignore variations across the thickness of the anode catalyst layer when considering the methanol concentration. We consider this assumption valid in this model because the catalyst layer is approximately an order of magnitude thinner than both the membrane and backing layer. Previous work [4–6,9] justifies this approach, as these papers show that, even at high current densities, the change in methanol concentration across a thin catalyst layer is much smaller than it is across either the membrane or the backing layer.

The methanol flux across the membrane is driven by diffusion and electroosmotic drag. Both forces will drive methanol toward the cathode, and the methanol flux density is

$$N_{\mathrm{MeOH}}^{mem} = -D_{mem}\frac{\partial c}{\partial x} + \frac{i\xi_{\mathrm{MeOH}}}{F}. \quad (4)$$

We assume that the electroosmotic drag of methanol is directly proportional to the methanol concentration, $\xi_{\mathrm{MeOH}} = \xi'_{\mathrm{MeOH}} \cdot c$; with these assumptions incorporated into the model, we can solve for the concentration profile in the membrane. The constant ξ'_{MeOH} is equivalent to the factor $\xi_{\mathrm{H_2O}}/c_{\mathrm{H_2O}}$, where $\xi_{\mathrm{H_2O}}$ is the drag coefficient for pure water and $c_{\mathrm{H_2O}}$ is the water concentration in a membrane exposed to pure liquid water. We assign values of $\xi_{\mathrm{H_2O}} = 2.5$ [30] and $c_{\mathrm{H_2O}} = 0.0546$ mol cm^{-3} [31] for pure water at 60 °C – neglecting the effect of changing methanol concentration – so that $\xi'_{\mathrm{MeOH}} = 46$ cm^3 mol^{-1}. The flux of methanol across the thickness of the membrane must be uniform at steady state, which implies that $\nabla \cdot N_{\mathrm{MeOH}}^{mem} = 0$. Therefore, the concentration profile is defined by

$$\frac{\partial^2 c}{\partial x^2} - \frac{i\xi'_{\mathrm{MeOH}}}{D_{mem}F}\frac{\partial c}{\partial x} = 0, \quad (5)$$

which after applying the boundary conditions $c = c_{anode}$ at $x = 0$ and $c = 0$ at $x = L_{mem}$, has the solution

$$c = \frac{c_{anode}}{1 - \exp[-\phi]}\left\{1 - \exp\left[\phi\left(\frac{x}{L_{mem}} - 1\right)\right]\right\}. \quad (6)$$

$\phi = (L_{mem}/D_{mem})(i\xi'_{\mathrm{MeOH}}/F)$ is a dimensionless ratio of the flux due to exclusively to electroosmotic drag at a reference concentration relative to the limiting value of the flux due to diffusion alone. As the plot in Fig. 2 shows, increasing the strength of the drag force relative to the diffusion force increases the amount of methanol in the membrane and stretches the concentration profile toward the cathode.

We have information about the rate at which methanol can move across the backing layer, and the rate at which any methanol that crosses the anode catalyst layer will move across the membrane, but we seek to describe these rates as a function of the two layers' transport and geometric properties, as well as the local value of the concentration in the flow channel. To simplify the mathematics from here, we define another dimensionless parameter n, which is a function of N_{MeOH}^{mem} and the constants L_{mem} and D_{mem}:

$$n = \frac{L_{mem}N_{\mathrm{MeOH}}^{mem}}{D_{mem}c_{anode}} = \frac{\phi \exp(\phi)}{\exp(\phi) - 1}. \quad (7)$$

n is a dimensionless ratio of the flux across the membrane subject to the operating conditions of the system relative to the value of the flux that would be present without electroosmotic drag. Now c_{anode} can be defined in terms of the cross over current i_x:

$$c_{anode} = \frac{i_x}{6Fn}\left(\frac{L_{mem}}{D_{mem}}\right). \quad (8)$$

Substituting c_{anode} back into Eq. (3), we can solve for i_x in a different form

$$i_x = (i_{\mathrm{lim}} - i)\left(\frac{\upsilon}{1 + \upsilon}\right), \quad (9)$$

where $\upsilon = (D_{mem}/L_{mem})(\phi\exp(\phi)/\exp(\phi) - 1)(L_{backing}/D_{backing})$ is a dimensionless ratio of the limiting current in the membrane relative to the limiting current in the backing layer. υ serves as a proxy for the amount of methanol that crosses over to the cathode.

For completeness, it should also be noted that substituting Eq. (4) for i_x into Eq. (9) and solving for c_{anode} produces a simple relationship between c_{anode} and c_{feed}.

$$c_{anode} = \left(1 - \frac{i}{i_{\mathrm{lim}}}\right)\left(\frac{1}{1 + \upsilon}\right) c_{feed}. \quad (10)$$

Further substitution of Eq. (2) for i_{lim} results the following expression for c_{anode}:

$$c_{anode} = \frac{\psi c_{feed} - c^0_{feed}}{\psi(1 + \upsilon)}. \quad (11)$$

This relationship is not used further in this paper, but it does show that c_{anode} is dependent on c_{feed} at the corresponding location in the flow channel, the initial feed concentration c^0_{feed}, the limiting current at the anode entrance normalized by the desired current $\psi = i^0_{\mathrm{lim}}/i$, and the dimensionless ratio υ.

2.3. Anode flow channel

Assuming the velocity v of methanol in the flow channel is constant, the total flow rate of methanol in the anode flow channel is given by

$$N_{\mathrm{MeOH}}^{channel} = c_{feed}\, A_{channel}\, v, \quad (12)$$

and the feed concentration down the channel is given by

$$\frac{\partial c_{feed}}{\partial z'} = -N_{\mathrm{MeOH}}^{backing}\left(\frac{w\, L_{channel}}{A_{channel}\, v}\right) = -\left(\frac{i + i_x}{6F}\right)\left(\frac{w\, L_{channel}}{A_{channel}\, v}\right), \quad (13)$$

where $z' = z/L_{channel}$ is the distance down the channel, and w is the channel separation width, that is, the width of electrode perpendicular to the channel flow that is fed by a single channel. $wL_{channel}$ is the area of the anode that receives the methanol flowing through the channel. The effects of other parallel channels are ignored.

While we allow for the crossover current i_x to vary with position, we make the simplifying assumption that current density i is independent of position along the anode flow field channel. While not strictly accurate, a cross-flow anode and cathode configuration and zero-order methanol kinetics suggest that local current densities are not a function of local methanol concentration and therefore might be treated as independent of position in the anode channel. This significantly simplifies the analysis and offers simplicity in examining the overall performance of the system.

After substituting Eq. (9) for i_x and applying the boundary condition $c_{feed}{}^0$ at $z=0$ with $\psi = i^0_{\lim}/i$, the solution to Eq. (12) is

$$c_{feed} = \left(c^0_{feed} + \frac{c^0_{feed}}{\upsilon\psi}\right)\exp\left(-\frac{\upsilon\psi}{s(1+\upsilon)}z'\right) - \frac{c^0_{feed}}{\upsilon\psi}. \quad (14)$$

A more useful formulation of the feed concentration is to define

$$\omega = \frac{c_{feed}}{c^0_{feed}} = \left(1+\frac{1}{\upsilon\psi}\right)\exp\left(-\frac{\upsilon\psi}{s(1+\upsilon)}z'\right) - \frac{1}{\upsilon\psi} \quad (15)$$

As a check on the reasonableness of this solution, we can find ω in the limit where the crossover (in this case represented by υ) goes to zero:

$$\lim_{\upsilon\to 0}\omega = 1 - \frac{z'}{s}. \quad (16)$$

As expected, ω is unity at $z'=0$ and goes to zero at the end of the channel. The parameter s in the equations above is defined as

$$s = \left(\frac{c^0_{feed}}{i/6F}\right)\left(\frac{A_{channel}\,\upsilon}{L_{channel}\,w}\right). \quad (17)$$

s is the stoichiometric ratio for the methanol flow: the rate at which methanol is delivered to the inlet of the cell relative to the amount of methanol that is consumed in the preferred electrochemical reaction. Hence, it represents the inverse of the fuel efficiency. This ratio is the critical point in this analysis, and in the following sections we use it to optimize the system-level fuel efficiency.

3. Fuel efficiency

3.1. Upper limit on fuel efficiency

In a region with sufficiently low methanol concentration at the anode, the anode potential must increase sharply in order to sustain a current as the methanol oxidation reaction transitions from zero-order to first-order [31]. Rather than model the complicated transition to first-order methanol kinetics, which would require a substantial overpotential at the anode and a corresponding loss in performance, we ensure that the optimized system remains above any such transition by requiring the feed concentration (represented by the dimensionless concentration ω) to remain above a minimum value throughout the flow channel. In doing so, we impose a constraint on the minimum allowable stoichiometric ratio s, which in turn constrains the values of υ and ψ. Fig. 4 reveals that if the stoichiometric ratio is too small, there will be no methanol in the flow channel at the stack exit ($z'=1$). This situation occurs when the system demands uniform current density beyond the point where the flow channel can supply methanol to the anode at a sufficient rate.

Returning to Eq. (3) relating i and i_x to c_{feed} and c_{anode}, we substitute Eq. (9) for i_x and c_{lim} for c_{anode} to find the feed concentration in terms of the minimum concentration c_{lim}:

$$\frac{c_{feed}}{c^0_{feed}} = \frac{c_{\lim}}{c^0_{feed}}(1+\upsilon) + \frac{1}{\psi} \text{ or } \omega = \theta(1+\upsilon) + \frac{1}{\psi}, \quad (18)$$

Table 1
Physical properties.

Parameter (unit)	Value	Reference
θ (dimensionless)	10^{-4}	Assumed
D_{MeOH-H_2O} ($cm^2\,s^{-1}$)	$10^{-1.416-999.778/T}$	Yaws [34]
ε (dimensionless)	0.7	Wang and Wang [29]
$D_{backing}$ ($cm^2\,s^{-1}$)	$D_{MeOH-H_2O}\,\varepsilon^{1.5}$ (base value)	Wang and Wang [29]
D_{mem} ($cm^2\,s^{-1}$)	4.9×10^{-6} (base value)	Kauranen and Skou [33]
$L_{backing}$ (cm)	0.0180 (base value)	Meyers and Newman [32]
L_{mem} (cm)	0.0179	Meyers and Newman [32]
c_{H_2O} ($mol\,cm^{-3}$)	0.0546	CRC Handbook [31]
ξ_{H_2O} (dimensionless)	2.5	Zawodzinski et al. [30]
ξ'_{MeOH} (dimensionless)	ξ_{H_2O}/c_{H_2O}	Calculated

where $\theta = c_{\lim}/c^0_{feed}$, which we set equal to 10^{-4} throughout this study. To find the maximum fuel efficiency that will accommodate this minimum feed concentration, we substitute Eq. (17) into Eq. (14), set $z'=1$ so that we are at the end of the channel, and solve for s. The result is

$$s \geq \frac{\upsilon\psi}{(1+\upsilon)\ln\left[(1+\upsilon\psi)/(1+\upsilon)\left(1+\theta\upsilon\psi\right)\right]}. \quad (19)$$

Placing this lower limit on s places an upper limit on fuel efficiency because efficiency (utilization) is $1/s$.

In order for s to be physically meaningful, it must be positive because all of the parameters that comprise it in Eq. (16) are positive definite. Therefore, the term inside the natural logarithm in the denominator must be greater than unity, which requires that $\psi > 1/(1-\theta-\upsilon \rightleftarrows \theta)$. This result makes sense if we reverse it to read $\theta+\upsilon\theta+1/\psi<1$. The term on the left is equal to ω as in Eq. (17). Because ω is the ratio of the feed concentration in the channel to the initial feed concentration, it must be less than unity. What we find is that for low feed concentrations, the current must be kept low or the backing layer must be very thin and porous. Otherwise, the anode concentration will not be kept above its minimum value (Table 1).

3.2. Optimization of backing layer properties for varying current loads

Now that we have a method for finding the maximum fuel efficiency under a given set of conditions, we can look to optimize the efficiency for the variety of current loads that the fuel cell must support. If fuel efficiency is the only concern, then the best choice is to lower the membrane permeability as much as possible and always pass a small current. However, the cell is always subject to a load requirement, and often that requirement varies.

In the following demonstration, we first optimize the fuel efficiency for a standard $0.05\,A\,cm^{-2}$ load by varying the limiting current of the backing layer. Then we adjust the limiting current based on the design constraint that the cell must be able to deliver high current ($0.5\,A\,cm^{-2}$ here) with reasonable efficiency while still staying close to the optimum efficiency at the standard load.

The width of the membrane is taken to be 0.0179 cm as in dry Nafion® 117 [32]. As a reference value for the diffusion coefficient in the membrane, and we refer to the superficial diffusivity measured by Kauranen and Skou [33]:

$$D_{mem} = 4.9\times10^{-6}\,cm^2\ \ s^{-1}\quad \text{at } 60^\circ C \quad (20)$$

Our reference point for the effective diffusion coefficient in the backing layer is taken from Wang and Wang [29], using their measured porosity of $\varepsilon = 0.7$ and the diffusion coefficient of methanol in

water $D_{MeOH-H_2O} = 10^{-1.416-999.778/T}$ cm^2 s^{-1} measured by Yaws [34]:

$$D_{backing} = D_{MeOH-H_2O}\,\varepsilon^{1.5} = 10^{-1.416-999.778/T}(0.7)^{1.5}\text{cm}^2\ \text{s}^{-1}$$
$$\text{or } 2.242\times10^{-5}\text{cm}^2\,\text{s}^{-1}\text{ at } 60^\circ\text{C}. \quad (21)$$

In each case, we fix the feed concentration at the channel input and vary the limiting current from just below the desired load value (0.05 A cm^{-2} and 0.5 A cm^{-2}) to twenty times that value. We then plot the maximum fuel efficiency as a function of the limiting current for a variety of feed concentrations. Referring to Eq. (2), the limiting current is directly proportional to the mass transfer coefficient $D_{backing}/L_{backing}$ when the initial feed concentration is fixed. Previous experimental work [3] has shown that the mass transfer coefficient can change with the methanol feed concentration in a two-phase regime, but the effect is small enough that we neglect it here.

Optimizing the fuel efficiency requires delivering enough methanol to the anode to produce the desired current without delivering so much that crossover to the cathode becomes a significant factor. Hence, the backing layer properties, which define the limiting current for a fixed methanol concentration, must be tuned to the membrane properties, the desired load, and the input methanol concentration. In both the high-current and the low-current cases, we can allow the limiting current to approach the load value, but the model will give nonphysical results if we demand a load higher than the limiting current.

The efficiency increases sharply until the limiting current reaches about four times the load value (0.2 A cm^{-2} in the low current case and 2 A cm^{-2} in the high current case) and then levels off or in some cases declines. In this scenario, operating the cell at a low feed concentration such as 0.1 M or 0.5 M with a limiting current at the anode of about 2 A cm^{-2} is optimal. The cell would run at its maximum efficiency during normal, low current operation while still maintaining reasonable efficiency when a higher load is demanded (Fig. 5)

3.3. Optimization of membrane properties

Now we can apply the same method to study how fuel efficiency is affected by changing the diffusion coefficient and the electroosmotic drag coefficient of the membrane. Looking back to Eq. (5), we see that these two material-based properties determine the methanol concentration profile in the membrane. First, we set the backing layer diffusion coefficient to 2.242×10^{-5}cm^2 s^{-1} as in Eq. (20) and the width of the backing layer to 0.0180 cm. Taking the width of the membrane to be 0.0179 cm as before and varying the diffusion coefficient from 5×10^{-9}cm^2 s^{-1} to 5×10^{-3}cm^2 s^{-1}, we can plot the fuel efficiency as a function of the diffusion coefficient and the input feed concentration as in Fig. 6(a) and (b). As expected, decreasing the membrane diffusion coefficient, which in effect lowers the crossover, has a dramatic positive effect on the fuel efficiency, especially in the low current case. The effect is more pronounced when the load is 0.05 A cm^{-2} because methanol is not being taken away as rapidly at the anode as it is in the 0.5 A cm^{-2} case.

Fig. 6(a) and (b) highlights again the cooperative effects of the membrane properties, backing layer properties and system configuration on the fuel efficiency. Altering the membrane diffusion coefficient has very little effect on the fuel efficiency except for a dramatic change in the region from 10^{-4} cm^2 s^{-1} to 10^{-6} cm^2 s^{-1}. Any changes in the fuel efficiency outside this region are limited by the chosen backing layer properties and the initial methanol concentration. The reader should also note that the data for input feed concentrations of 0.1 M and 0.5 M are not shown in Fig. 4(b). With the given set of backing layer properties at a 0.5 A cm^{-2} load, these concentrations result in negative fuel efficiencies. In other words,

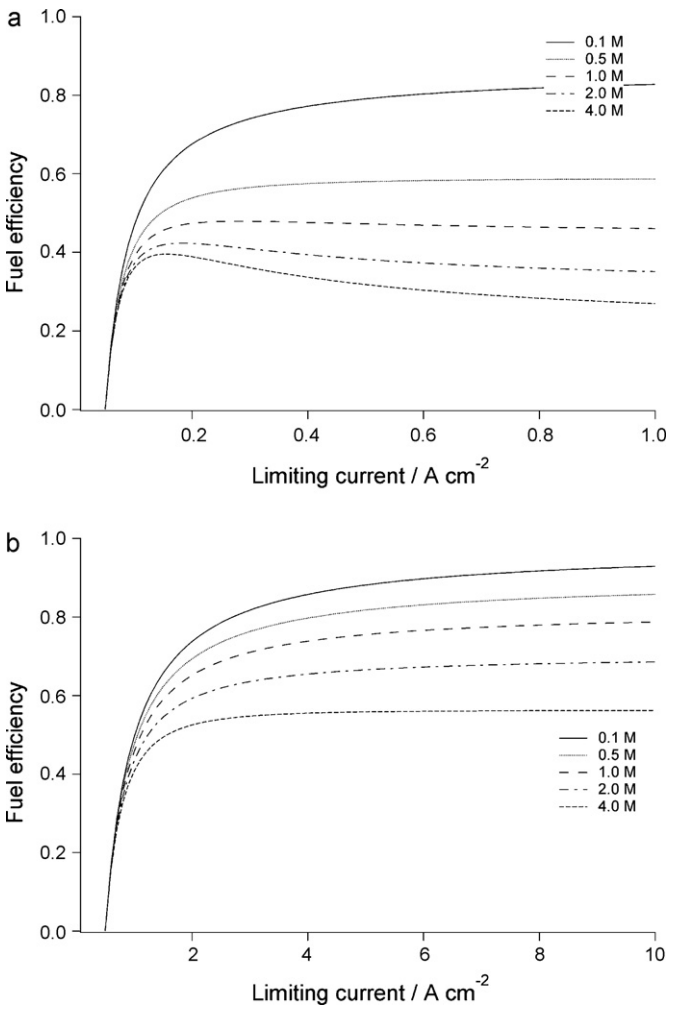

Fig. 5. (a) Maximum fuel efficiency as a function of limiting current with $I = 0.05$ A cm^{-2}. (b) Maximum fuel efficiency as a function of limiting current with $I = 0.5$ A cm^{-2}.

there is not sufficient methanol in the feed stream to sustain the desired current at the anode across the entire length of the fuel cell. The same goes for 0.1 M in Fig. 4(a), where there is barely enough methanol reaching the anode to sustain the desired current, resulting in low efficiency. Altering the membrane properties does not change this situation, so by this constraint we can rule out using these input feed concentrations to optimize the fuel efficiency.

Fixing the diffusion coefficient at the reference value of 4.9×10^{-6}cm^2 s^{-1} given in Eq. (19), we now vary the methanol drag coefficient $\xi'_{MeOH} = \xi_{H_2O}/c_{H_2O}$ to gauge its effect on the fuel efficiency. For demonstration purposes we arbitrarily choose to vary the value of ξ'_{MeOH} over a wide range, from 0.1 to 10^5 cm^3 mol^{-1}. Recalling Fig. 2 should give us a hint at the results. Increasing the drag coefficient by a factor of twenty noticeably increases the extent of methanol crossover in the membrane, which should decrease fuel efficiency. Given that we are varying the drag coefficient by a factor of 10^6, we should see substantial changes in the fuel efficiency.

However, Fig. 7(a) and (b) shows the maximum fuel efficiency changes very little until $\xi'_{MeOH} > 500$ cm^3 mol^{-1} in the low current case and $\xi'_{MeOH} > 50$ cm^3 mol^{-1} in the high current case. Measurements of the water drag coefficient in a variety of DMFC membranes range from $\xi_{H_2O} = 2$ to $\xi_{H_2O} = 5$ depending on temperature and the equivalent weight of the membrane [35]. These values correspond to a range of $\xi'_{MeOH} = 36$ cm^3 mol^{-1} to $\xi'_{MeOH} = 80$ cm^3 mol^{-1}, which includes the reference value of $\xi'_{MeOH} =$

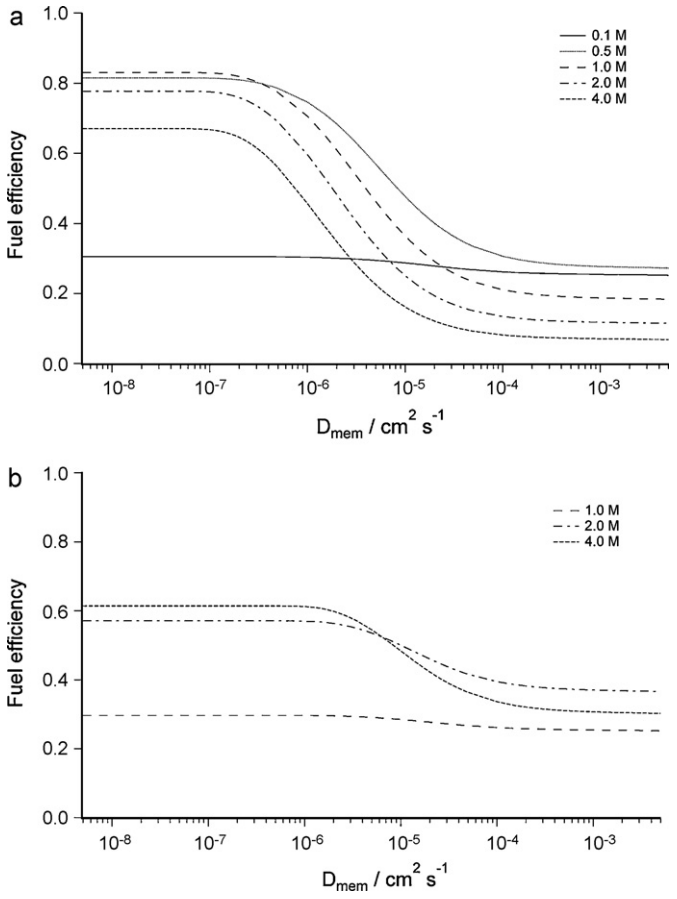

Fig. 6. (a) Maximum fuel efficiency vs. membrane diffusion coefficient for varying feed concentrations and $I = 0.05\ \mathrm{A\,cm^{-2}}$. (b) Maximum fuel efficiency vs. membrane diffusion coefficient for varying feed concentrations and $I = 0.5\ \mathrm{A\,cm^{-2}}$.

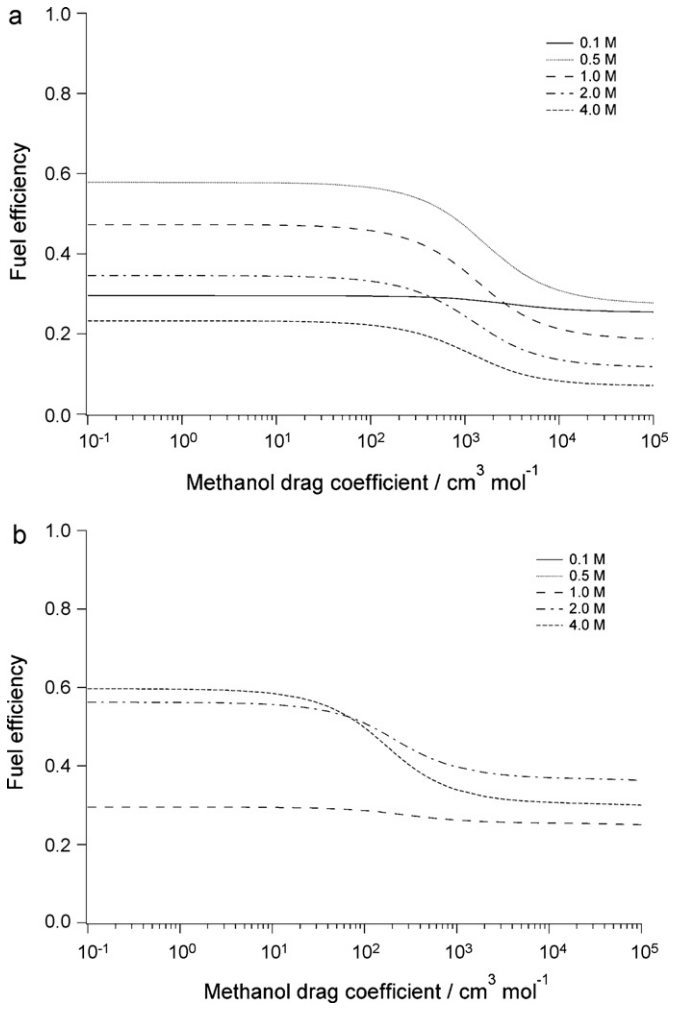

Fig. 7. (a) Maximum fuel efficiency vs. methanol drag coefficient for varying feed concentrations and $I = 0.05\ \mathrm{A\,cm^{-2}}$. (b) Maximum fuel efficiency vs. methanol drag coefficient for varying feed concentrations and $I = 0.5\ \mathrm{A\,cm^{-2}}$.

46 $\mathrm{cm^3\ mol^{-1}}$ given in Section 2.2. In other words, the drag coefficient or the current must be very high in order for electroosmotic drag to affect efficiency as much as diffusion does. The expected trend of decreasing fuel efficiency for increasing drag does exist, but the effect of drag is minimal within the range of physically reasonable ξ'_{MeOH} values, especially in the low current case. At low current densities, the given membrane and backing layer properties must be altered if the drag is to have a greater effect on the fuel efficiency.

Throughout this analysis and especially in this section, it is important to remember that this model is concerned only with *fuel* efficiency and not *system* efficiency. System efficiency is a more complete measure of fuel cell performance because it is a product of the reversible thermodynamic efficiency (for an ideal fuel cell), the voltage efficiency (incorporating kinetic losses), and the fuel efficiency. Optimizing the fuel efficiency is not always correlated to optimizing the voltage efficiency, so achieving maximum fuel efficiency does not guarantee maximum system efficiency. Only in applications where portability takes precedence over power output is fuel efficiency of primary concern, and it is those applications that this model is most useful in system design. Keeping this point in mind, the next section will consider how to estimate the required size of system components for a fuel cell operating at its maximum fuel efficiency.

4. Methanol flux and the size of system components

Because portability is of primary importance in many applications where DMFCs might be used, we want to use this model to predict how large the methanol storage tank, circulation pump, cell stack, and other components need to be to produce a required methanol flow rate. The less methanol that is used and the more slowly it is passed through the anode channel, the smaller we can make these various system components. However, a minimum flow rate is set by the current that the cell must generate. Ideally, there would be no methanol crossover, and all of the fuel in the system would either be consumed in the desired reaction or recirculated through the system to be consumed later; the size of the fuel tank would be solely dependent on the demand for current. However, the existence of crossover and the potential for wasted fuel means that the size of the tank also depends on the fuel efficiency.

First, lets consider the size of the methanol storage tank in a situation where the fuel is not recycled. The minimum flow rate into the anode channel needed to produce the required feed concentration is

$$N_{\mathrm{MeOH}}^{input} = c_{feed}^{0} A_{channel}\, v = \frac{iA}{6F} s, \tag{22}$$

where A is the electrode area, which is equal to $w \cdot L_{channel}$. In this case, the input flow rate or flux is directly proportional to the stoichiometric ratio and therefore inversely proportional to the fuel efficiency. The size of the fuel tank and the circulation pump are in turn proportional to the flow rate. Therefore, we can employ the analysis used in Section 3 to maximize the fuel efficiency and thereby minimize the size of the fuel tank and circulation pump.

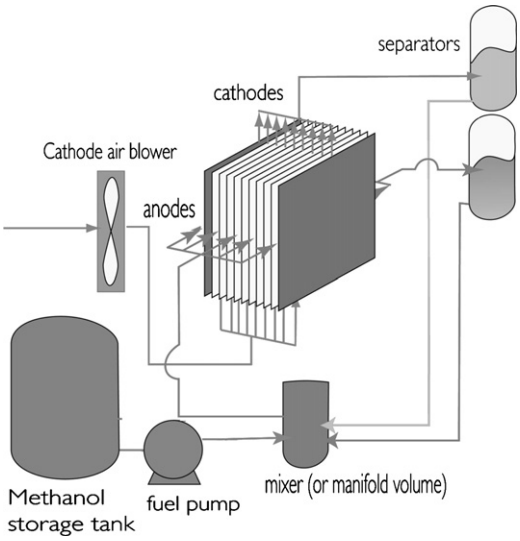

Fig. 8. Schematic of the entire fuel cell system.

Now we consider a scenario, depicted in Fig. 8, where the methanol/water solution is separated from the carbon dioxide at the stack exit and is recirculated through the system. The output flux from the anode channel is the input flux minus the flux that is redirected into the cell. The value of ω at the stack exit represents the fraction of methanol that is consumed in the entire cell, so multiplying the input flux by ω gives us the output flow rate

$$N_{\mathrm{MeOH}}^{output} = \frac{iA}{6F} s \left(\theta + \upsilon\theta + \frac{1}{\psi} \right). \tag{23}$$

The required flow rate of methanol from the storage tank into the fuel system is the input flow rate minus the output flow rate:

$$N_{\mathrm{MeOH}}^{\mathrm{tank}} = \frac{iA}{6F} s \left(1 - \theta - \upsilon\theta - \frac{1}{\psi} \right) \tag{24}$$

In this case, the stoichiometric ratio is not the only parameter that determines the methanol flow rate and the size of the fuel tank. Fig. 9(a) and (b) plots the flux – without including the area of the anode A as is shown above – as a function of the limiting current for a system with recirculation. Two points must be considered when looking at these plots. First, the plots cut off when the limiting current reaches the desired current because allowing the limiting current to reach or to fall below the desired current will produce a nonphysical result. Also note that increasing the load requirement by a factor of ten increases the required methanol flux from the storage tank by a factor ranging from about five to ten. Designing a fuel delivery system that can handle such a wide range of methanol flow rates is an important engineering problem that this model forecasts but of course does not answer.

An important question that this analysis can answer is the question of whether a recirculation system is needed. Comparing Fig. 9(a) and (b) to Fig. 5(a) and (b) demonstrates the differences in required methanol flux between a system with recirculation and a system where the flux depends solely on the efficiency. In both the high and low current scenarios with recirculation, the flux – and consequently the tank size – increases as the anode limiting current increases. Without recirculation, the trend is the opposite. Therefore, one can consider the tradeoffs of a recirculation system once one knows the duration of operation and scaling of pump sizes and tank sizes with total capacity. If the optimum conditions for the system dictate that very little fuel comes out of the stack, then the separators and pumps may be a waste of important space and power in a portable device.

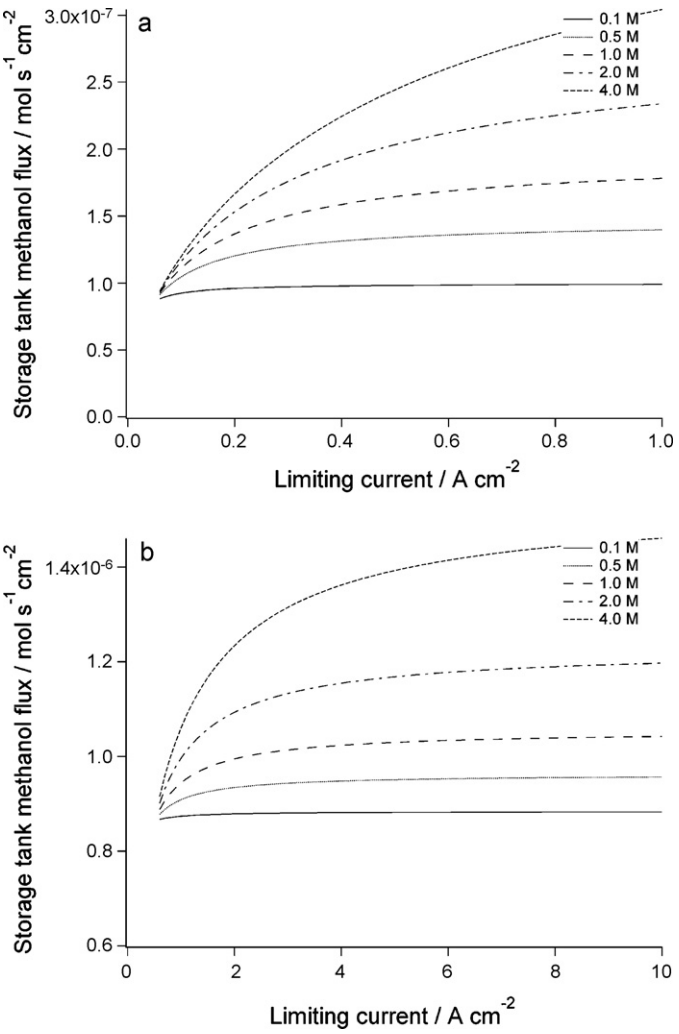

Fig. 9. (a) Storage tank flux as a function of limiting current with $I = 0.05\ \mathrm{A\,cm^{-2}}$. (b) Storage tank flux as a function of limiting current with $I = 0.5\ \mathrm{A\,cm^{-2}}$.

5. Conclusion

Using analytic calculations of the methanol concentration, it is possible to illustrate the effects of material properties and system design on the fuel efficiency of the direct methanol fuel cell. Fuel efficiency can be calculated by taking the ratio of the amount of methanol that enters the cell to the amount that is consumed in the desired reaction. By requiring the stoichiometric ratio to be maintained above a minimum value at the stack exit, a maximum achievable fuel efficiency can be calculated. Optimizing the fuel efficiency based on the limiting current at the anode requires matching the backing layer properties to the feed concentration and to the load requirement. Lowering the diffusion coefficient in the membrane always improves the fuel efficiency by lowering methanol crossover, especially in the low current scenario. Altering the electroosmotic drag coefficient of methanol in the membrane has very little effect on the fuel efficiency unless either the current or the drag coefficient is very high. The size of system components can also be calculated based on the required methanol flux into and out of the cell operating at maximum efficiency. Generally speaking, the size of the fuel tank and other components decreases as the feed concentration and load requirements decrease.

While this model does not allow for tradeoffs of power versus energy or the likely tradeoff between ohmic losses and crossover in the membrane, future work may incorporate electrochemical equa-

tions into this model so that it can make predictions about power output and other performance parameters that are important in real fuel cell systems. Such an addition would add complexity to the model but give it more relevance to experimental data. Despite the model's limitations, it does give insights into designing a fuel cell system for maximum fuel efficiency across a dynamic current range. It also offers pathways to more complex and realistic modeling that is of interest to scientists seeking to maximize fuel cell performance.

Acknowledgement

Financial support by the Office of Naval Research MURI grant no. N00014-07-1-0758 is gratefully acknowledged.

References

[1] K. Scott, W. Taama, J. Cruickshank, J. Power Sources 65 (1997) 159–171.
[2] J. Cruicksahank, K. Scott, J. Power Sources 70 (1998) 40–47.
[3] K. Sundmacher, K. Scott, Chem. Eng. Sci. 54 (13–14) (1999) 2927–2936.
[4] K.T. Jeng, C.W. Chen, J. Power Sources 112 (2002) 367–375.
[5] A.A. Kulikovsky, Electrochem. Commun. 4 (2002) 939–946.
[6] A.A. Kulikovsky, Electrochem. Commun. 5 (2003) 530–538.
[7] K. Scott, P. Argyropoulos, J. Power Sources 137 (2) (2004) 228–238.
[8] K. Scott, P. Argyropoulos, J. Electroanal. Chem. 567 (2004) 103–109.
[9] B.L. García, V.A. Sethuraman, J.W. Weidner, R.E. White, J. Fuel Cell Sci. Technol. 1 (2004) 43–48.
[10] R. Chen, T.S. Zhao, J. Power Sources 152 (2005) 122–130.
[11] A.A. Kulikovsky, Electrochim. Acta 53 (3) (2007) 1353–1359.
[12] V.B. Oliveira, D.S. Falcão, C.M. Rangel, A.M.F.R. Pinto, Int. J. Hydrogen Energy 33 (2008) 3818–3828.
[13] D. Kareemulla, S. Jayanti, J. Power Sources 188 (2009) 367–378.
[14] M.A. Mosquera, W.H. Lizcano-Valbuena, Electrochim. Acta 54 (2009) 1233–1239.
[15] H. Guo, C.-F. Ma, Electrochem. Commun. 6 (2004) 306–312.
[16] S.L. Ee, E. Birgersson, J. Electrochem. Soc. 156 (11) (2009) B1329–B1338.
[17] J.P. Meyers, J. Newman, J. Electrochem. Soc. 149 (6) (2002) A729–A735.
[18] L. Xianglin, H. Yaling, Y. Benhao, M. Zheng, L. Xiaoyue, J. Power Sources 178 (1) (2008) 344–352.
[19] A. Casalegno, R. Marchesi, J. Power Sources 185 (2008) 318–330.
[20] I. Jeong, J. Kim, S. Pak, S. Nam, I. Moon, J. Power Sources 185 (2008) 828–837.
[21] D.H. Ko, M.J. Lee, W.H. Jang, U. Krewer, J. Power Sources 180 (2008) 71–83.
[22] C. Xu, P.M. Follmann, L.T. Biegler, M.S. Jhon, Comput. Chem. Eng. 29 (2005) 1849–1860.
[23] V.S. Silva, A. Mendes, L.M. Madeira, S.P. Nunes, J. Membr. Sci. 276 (2006) 126–134.
[24] D. Ye, X. Zhu, Q. Liao, J. Li, Q. Fu, J. Power Sources 192 (2009) 502–514.
[25] C. Cho, Y. Kim, Y.S. Chang, J. Thermal Sci. Technol. 4 (3) (2009) 414–423.
[26] J. Ko, P. Chippar, H. Ju, Energy 35 (2010) 2149–2159.
[27] P. Chippar, J. Ko, H. Ju, Energy 35 (2010) 2301–2308.
[28] K. Scott, W. Taama, J. Cruickshank, J. Appl. Electrochem. 28 (1998) 289–297.
[29] Z.H. Wang, C.Y. Wang, J. Electrochem. Soc. 150 (4) (2003) A508–A519.
[30] T.A. Zawodzinski, J. Davey, J. Valerio, S. Gottesfeld, Electrochim. Acta 40 (3) (1995) 297–302.
[31] W.M. Haynes (Ed.), CRC Handbook of Chemistry and Physics (Internet version), 91st ed., CRC Press/Taylor and Francis, Boca Raton, FL, 2011.
[32] J.P. Meyers, J. Newman, J. Electrochem. Soc. 149 (6) (2002) A718–A728.
[33] P.S. Kauranen, E. Skou, J. Appl. Electrochem. 26 (1996) 909–917.
[34] C.L. Yaws, Handbook of Transport Property Data: Viscosity, Thermal Conductivity, and Diffusion Coefficients of Liquids and Gases , Gulf Pub. Co., Houston, TX, 1995.
[35] X. Ren, S. Gottesfeld, J. Electrochem. Soc. 148 (1) (2001) A87–A93.

Glossary

i: current through the external circuit ($A\,cm^{-2}$)
i_x: crossover current ($A\,cm^{-2}$)
i_{lim}: limiting current in the backing layer ($A\,cm^{-2}$)
i^0_{lim}: backing layer limiting current at channel inlet ($C\,cm^{-2}\,s^{-1}$)
ψ: ratio of i^0_{lim} to the current through the external circuit (dimensionless)
υ: ratio of limiting current in backing layer and membrane (dimensionless)
c_{anode}: methanol concentration at the anode ($mol\,cm^{-3}$)
c_{feed}: methanol concentration in the feed stream ($mol\,cm^{-3}$)
c^0_{feed}: feed concentration at channel inlet ($z = 0$) ($mol\,cm^{-3}$)
ω: ratio of c_{feed} at distance z compared to at $z = 0$ (dimensionless)
c_{lim}: minimum methanol concentration at the anode ($mol\,cm^{-3}$)
c_{H_2O}: concentration of water in the membrane ($mol\,cm^{-3}$)
θ: ratio of c_{lim} to c^0_{feed} (dimensionless)
$D_{backing}$: effective diffusion coefficient in the backing layer ($cm^2\,s^{-1}$)
ε: porosity of the backing layer (dimensionless)
D_{MeOH-H_2O}: diffusion coefficient of methanol in water ($cm^2\,s^{-1}$)
D_{mem}: diffusion coefficient in the membrane($cm^2\,s^{-1}$)
$L_{backing}$: width of the backing layer (cm)
L_{mem}: width of the membrane (cm)
$N^{backing}_{MeOH}$: flux of methanol through the backing layer ($mol\,cm^{-2}\,s^{-1}$)
N^{mem}_{MeOH}: flux of methanol through the membrane ($mol\,cm^{-2}\,s^{-1}$)
$N^{channel}_{MeOH}$: flux of methanol through the flow channel ($mol\,cm^{-2}\,s^{-1}$)
ξ_{MeOH}: electroosmotic drag factor of methanol (dimensionless)
ξ'_{MeOH}: electroosmotic drag coefficient of methanol ($cm^3\,mol^{-1}$)
ξ_{H_2O}: electroosmotic drag coefficient of water ($cm^3\,mol^{-1}$)
ϕ: ratio of flux due to drag relative to diffusion (dimensionless)
n: mathematical construct (no physical meaning) (dimensionless)
w: flow channel separation width (cm)
z: distance down the flow channel (cm)
z': normalized distance down the flow channel (dimensionless)
s: stoichiometric ratio for the methanol flow (dimensionless)
$A_{channel}$: cross-sectional area of the flow channel (cm^2)
A: superficial area of the anode (cm^2)
N^{input}_{MeOH}: methanol flux into the cell ($mol\,cm^{-2}\,s^{-1}$)
N^{output}_{MeOH}: methanol flux out of the cell ($mol\,cm^{-2}\,s^{-1}$)
N^{tank}_{MeOH}: methanol flux out of the tank ($mol\,cm^{-2}\,s^{-1}$)